RAPID COMMUNICATIONS

PHYSICAL REVIEW B **91**, 220507(R) (2015)

Comparison of pressurized sulfur hydride with conventional superconductors

E. J. Nicol[1,*] and J. P. Carbotte[2,3]

[1]*Department of Physics, University of Guelph, Guelph, Ontario N1G 2W1, Canada*
[2]*Department of Physics and Astronomy, McMaster University, Hamilton, Ontario L8S 4M1, Canada*
[3]*The Canadian Institute for Advanced Research, Toronto, Ontario M5G 1Z8, Canada*

(Received 19 April 2015; revised manuscript received 10 June 2015; published 26 June 2015)

A recent report that sulfur hydride under pressure is an electron-phonon superconductor with a T_c of 190 K has been met with much excitement although it is yet to be confirmed. Based on several electron-phonon spectral density functions already available from density functional theory, we find that the electron-phonon spectrum is near optimum for T_c with a particularly large value of its characteristic phonon energy $\omega_{\ln}$ which is due to the small hydrogen mass. We find that the thermodynamic universal BCS ratios are near those for Pb and Nb_3Sn. We suggest that optical measurements could be a useful tool to establish the existence and nature of the superconductivity in this system. Conventional superconductors are in the impurity-dominated dirty limit. By contrast sulfur hydride will be in the clean limit because of its large energy gap scale. The ac optical conductivity will display distinct and separate signatures of the superconducting gap in the low-energy impurity-dominated range of the optical spectrum and additional phonon structures at higher energies where the clean limit applies.

DOI: 10.1103/PhysRevB.91.220507 PACS number(s): 74.20.Fg, 74.20.Pq, 74.25.Gz, 74.62.Fj

The observation [1] of a dramatic and sharp drop in resistivity around a temperature of $T \lesssim 190$ K in a sulfur hydride sample under ~ 200 GPa, has led to a flurry of new theoretical works [2–8]. The verification that it is definitely superconducting, for example through the observation of a Meissner effect, still awaits further experiments; however, the authors did observe that with the application of a magnetic field of 7 T there was a shift, to lower temperature, of the onset of the resistivity drop by ~ 10 K. Moreover, the conductivity below 190 K was found to be better than that of the purest metal at low temperature and was two orders of magnitude larger than that of pure copper.

A number of papers [2–4] based on density functional theory for sulfur hydride have already provided detailed information on the electron-phonon spectral density function $\alpha^2F(\omega)$ and have identified H_3S as the most likely phase involved at that pressure. While some quantitative differences exist between the various spectral densities available, all calculations support the idea of phonon-mediated superconductivity in H_3S with a T_c of order 200 K at ~ 200 GPa. Still it remains essential to find ways to directly verify such a possibility. Lacking definitive confirmation, it is instructive to place H_3S within the context of the family of known conventional superconductors [9]. In particular, an emphasis on differences and commonalities between H_3S and the well-established cases of electron-phonon-mediated superconductivity can provide valuable insight. It is also important to calculate the expected properties of the superconducting state of H_3S with the specific aim of providing information that can be used by experimentalists to establish that H_3S is indeed a superconductor and to discover the pairing mechanism involved, i.e., the glue that binds the Cooper pairs.

In this Rapid Communication, we demonstrate that H_3S is a very highly optimized electron-phonon superconductor for various reasons and we provide a calculation of the optical conductivity as a test for identifying the superconducting gap and the Holstein structure for the phonon spectrum. For this purpose, we work with the $\alpha^2F(\omega)$ spectrum provided in the literature. For illustrative purposes we have used the one developed by Errea *et al.* [3] (shown in Fig. 1) which includes anharmonic phonon effects. However, in the Supplemental Material [10] (Fig. S1), we also show the spectra for the harmonic version from Errea *et al.* along with that from Flores-Livas *et al.* [4] for comparison (the one from Duan *et al.* [2] is also similar but not shown). Using the $\alpha^2F(\omega)$, one can calculate the electron-phonon mass renormalization parameter, $\lambda = \int_0^\infty [\alpha^2F(\omega)/\omega]d\omega$, the area under the spectrum $A = \int_0^\infty \alpha^2F(\omega)d\omega$ and the Allen-Dynes characteristic phonon frequency [11,12] $\omega_{\ln} = \exp\{(2/\lambda)\int_0^\infty [\ln(\omega)\alpha^2F(\omega)/\omega]d\omega\}$, which would equal ω_E if the $\alpha^2F(\omega) = A\delta(\omega-\omega_E)$. For our digitization of the published spectrum shown in Fig. 1, $\lambda = 1.67$, $A = 118.5$ meV, and $\omega_{\ln} = 122$ meV. Comparison of these characteristic properties with the other spectra are given in Table S1 of the Supplemental Material [10]. (Note, these spectra were digitized from the original papers and placed on a 2 meV grid. This gives characteristics that are in qualitative agreement with the original works if not always in perfect quantitative agreement. Such details do not impact our results and conclusions presented here. It is clear that all of the spectra are qualitatively similar [10]). Calculating T_c with these spectra using the standard s-wave electron-phonon Eliashberg equations [9], we find that for $T_c = 190$ K, the Coulomb pseudopotential μ^* would have to be 0.18 for the anharmonic spectrum and about 0.38–0.4 for the harmonic spectrum (or conversely, for a $\mu^* \sim 0.16$, the harmonic spectra would give a T_c of order 250 K, which has been noted by the authors of these spectra). While a large μ^* is unusual, such a value has been found for the alkali-doped fullerenes [13] and can be taken as an argument for strong electron correlations to be important in addition to the electron-phonon interaction. It should be noted that the spectrum of Flores-Livas is one that has been developed and used by accounting for a nonconstant energy-dependent electronic density of states and yet it essentially agrees with the Errea harmonic spectrum. These details aside and working with the anharmonic spectrum

---

[*] enicol@uoguelph.ca

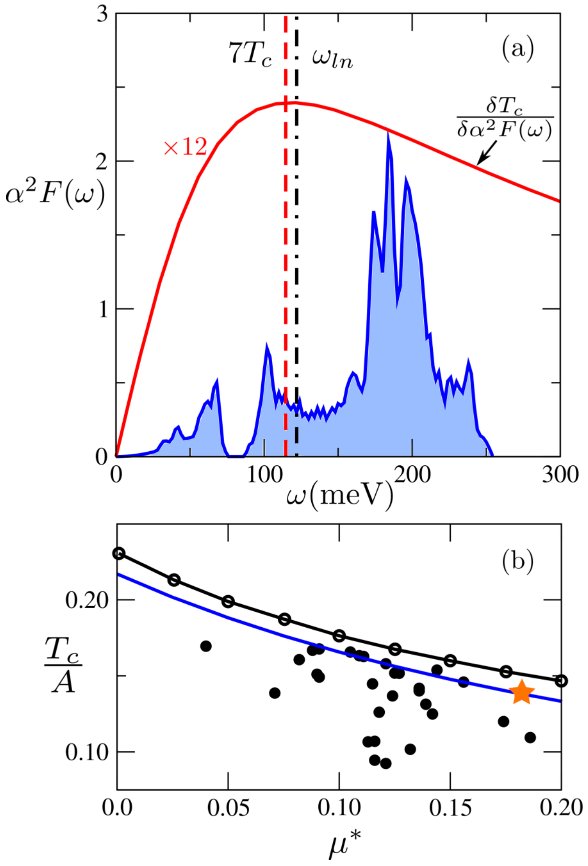

FIG. 1. (Color online) (a) The anharmonic $\alpha^2F(\omega)$ spectrum for H_3S at 200 GPa given in Ref. [3]. The functional derivative $\delta T_c/\delta\alpha^2F(\omega)$ vs ω for this same spectrum is also shown scaled up by a factor of 12. It peaks at $\omega = 7k_BT_c$ (dashed line) which is very close to the characteristic phonon frequency $\omega_{\ln}$ (dash-dotted line) for the $\alpha^2F(\omega)$ demonstrating that the spectrum is highly optimized for T_c. (b) T_c/A vs μ^* where A is the area under the $\alpha^2F(\omega)$ spectrum. The black curve with open circles is the theoretical upper limit for T_c with fixed A and the solid circles are data for several superconductors constructed from Table IV of Ref. [9]. The gold star is for the $\alpha^2F(\omega)$ spectrum in (a) with $T_c = 190$ K and $\mu^* = 0.18$. The blue curve represents how T_c/A would change for varying μ^*, demonstrating that this spectrum is near optimal.

for illustration, we argue that the $\alpha^2F(\omega)$ for H_3S is one of the most highly optimized among conventional superconductors.

One test of this concept is to evaluate the functional derivative of T_c (Ref. [14]) with respect to this spectrum as is shown in Fig. 1(a) (red curve). This derivative is peaked at $\omega \sim 7k_BT_c$ and illustrates that if one could move all the spectral weight in the $\alpha^2F(\omega)$ to a delta function placed at this frequency, then one would obtain the highest T_c possible from this spectrum. However, the spectrum is distributed around this point and so the question remains as to how optimized it is. Using the characteristic phonon energy $\omega_{\ln}$ as a measure, one finds that it is very close to the value of $7T_c$ as shown in the figure. Consequently, the spectrum is quite highly optimized already. This is understood from the fact that the functional derivative varies quite slowly about its peak and much of the weight of the $\alpha^2F(\omega)$ falls in the region of this slow variation. The shape of the functional derivative speaks to the physics that for phonon frequencies that are too low, the phonons do not respond fast enough to pair the electrons, but rather act more like static impurities. Alternatively, at very high frequencies, the ions would wiggle too fast to have any net displacement or polarization to glue the Cooper pairs. As a result, the optimal frequency is found at some intermediate frequency. A simple physical argument for the maximum to occur at $\omega \sim 7k_BT_c$ can be found in Refs. [9,15].

The question as to how optimal this spectrum is can be quantified by examining Fig. 1(b) where the dimensionless ratio of T_c/A is plotted versus μ^*. The line with the open circles is the maximum value that T_c could take for fixed A as a function of μ^* and is calculated by placing a delta function of weight A at the frequency of the peak in its own functional derivative and finding the T_c. This is a classic curve taken from Leavens [16] and the solid black dots represent the data for several conventional superconductors taken from a tabulation (Table IV) in Ref. [9]. The gold star shows where the spectrum in Fig. 1(a) sits and it is just below the optimal line. Indeed, it falls only 8% below the theoretical absolute upper bound allowed to any spectrum with that area A and μ^*. Furthermore, the blue curve shows how T_c would vary for this spectrum as a function of μ^* and it is clear that it would always remain close to the upper bound. For $\mu^* = 0$, the $T_c = 298$ K.

One may now try to understand from this why the T_c is so high. It is the unusually large value of A in H_3S which accounts for the large T_c found in this system. This sizable A comes about because the electron-ion coupling remains large to very high phonon energies. In turn, the unusually large value of $\omega_{\ln}$ is traced to the small hydrogen mass and the stiffness of the H-S bond stretching mode. Moreover, the lack of an electronic core structure to the hydrogen (see particularly Ref. [4]) means that there is no orthogonalization of the conduction electron wave functions which in ions with core electrons effectively changes the electron-ion interaction potential into a weakened pseudopotential. These two facts combined provide the mechanism for a large area A under the spectral density $\alpha^2F(\omega)$ which extends to high energies with large magnitude. Further insight into the importance of a large $\omega_{\ln}$ can be obtained through an analysis based on the asymptotic formula [9] for T_c of Eliashberg theory derived on the assumption of a very large value of λ, the mass enhancement factor. In this limit $T_c = 0.182\sqrt{\lambda}\omega_{\ln}$. We see that increasing λ by a factor of 2 increases T_c by $\sim$40%, while increasing $\omega_{\ln}$ by 2 doubles the T_c. While H_3S is not in the asymptotic limit of large λ, this analysis nevertheless provides a useful qualitative picture. While λ for H_3S is not particularly large as compared with other electron-phonon superconductors, $\omega_{\ln}$ is quite significant at about 120 meV. Through the numerical solution of the Eliashberg equations for many model spectra, Leavens and Carbotte [17] observed that, for λ and μ^* in the range of $1.2 < \lambda < 2.4$ and $0.1 < \mu^* < 0.15$, a remarkably simple relationship between T_c and A applied, namely, $T_c = 0.148A$. This formula can be used to obtain further understanding of the role various regions of the $\alpha^2F(\omega)$ spectrum play in T_c. As an example, the entire region below $\sim$165 meV in the spectrum of Fig. 1(a) has an area of 39 meV, while the area above is 80 meV, contributing, respectively, 67 and 137 K to the T_c value. It is clear that the hydrogen bending vibrations and most importantly the

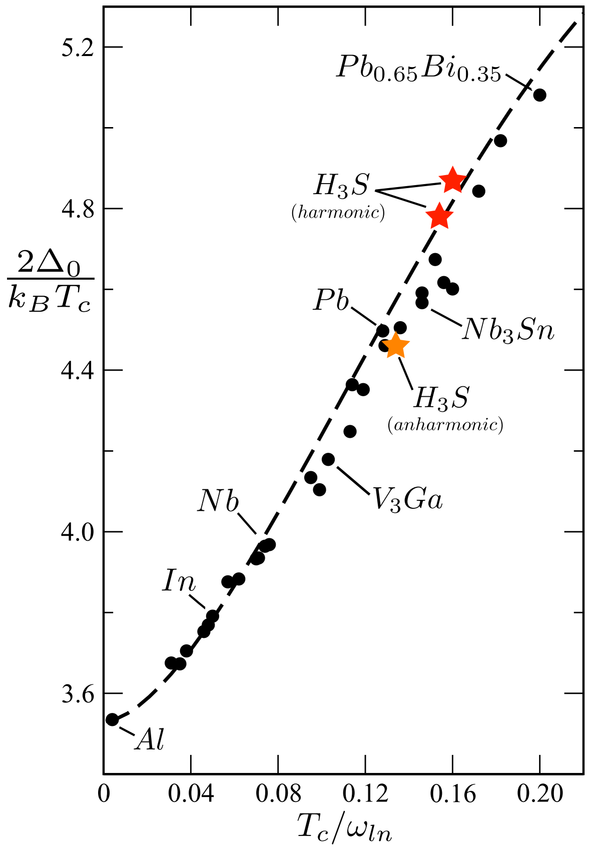

FIG. 2. (Color online) The gap ratio $2\Delta_0/k_B T_c$ vs $T_c/\omega_{\ln}$. The solid black points are the data for several conventional superconductors taken from Table IV of Ref. [9]. Some have been labeled. The dashed line is an analytical formula developed for conventional superconductors from strong coupling Eliashberg theory [18]. The gold star is the value calculated for the anharmonic spectrum shown in Fig. 1 and the red stars are the values for the harmonic spectra [10] with $T_c = 190$ K.

stretching modes are critical for the high T_c of H_3S metallic phase.

In Fig. 2, we compare the gap ratio calculated for sulfur hydride with other conventional superconductors on a classic plot [18,19] for the gap ratio versus $T_c/\omega_{\ln}$. We have done this calculation for both the anharmonic spectrum (gold star) and the two harmonic spectra shown in the Supplemental Material [10] (with $T_c = 190$ K). Clearly, sulfur hydride fits well among the conventional superconductors and sits close to Pb and Nb_3Sn which are other highly optimized superconductors. Using this figure one can also translate to other figures for strong coupling corrections to BCS ratios as found in Refs. [9,20]. We have done the numerical calculation and find for the anharmonic spectrum the specific heat ratio $\Delta C(T_c)/\gamma T_c = 2.53$ and the magnetic field ratio $\gamma T_c^2/H_c^2(0) = 0.136$, which are very close to the values found for Pb, as expected from Fig. 2.

We conclude from this that sulfur hydride appears to be a very highly optimized electron-phonon superconductor which uses the high phonon frequency of the hydrogen and large electron-ion interaction to obtain a high T_c. Nonetheless, it remains a question as to how to demonstrate the superconductivity and verify the electron-phonon interaction. Given that the sample is under pressure, many typical experimental probes may not be used. Tunneling was the classic experiment in conventional superconductors but here the energy scales are much higher than those that are usually accessed with tunneling. Consequently, an experiment which is noncontact but can probe high energy scales is needed. Here one is further helped by the fact that the material will be in the “clean limit,” where $2\Delta_0 \gg 1/\tau$ with $1/\tau$ being the impurity scattering rate [21]. An excellent probe in this case, then, is optical conductivity measurements as they may be done on a sample in a high pressure cell. As the cuprate superconductors have already illustrated, the clean limit allows one to see boson structure in optics [22]. This is illustrated in Fig. 3 where we show our calculation for the optical conductivity for the anharmonic spectrum of H_3S. [A comparison with that from the other $\alpha^2F(\omega)$ spectra is given [10] in Fig. S2]. Shown are the superconducting and normal state curves for $T = 0.1T_c$. In the latter case, Δ is set to zero in the calculation [21] and this curve is shown at the same temperature to illustrate differences between the two states independent of temperature. (For the normal state at T_c, which is not that different, see Fig. S3 of the Supplemental Material [10].) While the normal state shows a Drude absorption followed by a bump associated with the main source of inelastic scattering from the 200 meV peak in the electron-phonon spectrum (see Fig. 1), the superconducting state is much more dramatic. Here one sees a sharp impurity-dominated peak at the gap edge of $2\Delta_0 = 73$ meV and then a series of absorption peaks. This structured absorption can be traced to the $\alpha^2F(\omega)$ spectrum which we show in Fig. 3 shifted along the frequency axis by $2\Delta_0$. A full analysis and inversion [23] is needed to pull out the $\alpha^2F(\omega)$ from the data, but it is clear that there are signatures of the energy gap, phonon structures, and a shift in the main absorption hump going from the normal state to the superconducting state. By referring [10] to Fig. S3 for temperature-dependent spectra, it can be seen that such structures and overall response survive up to very high temperature and are quite robust. As a final note, for these calculations we have used a transport

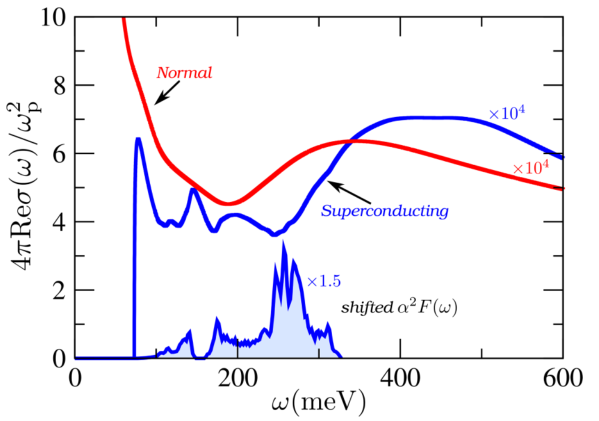

FIG. 3. (Color online) The real part of the optical conductivity (scaled up by a factor of 10^4) vs ω at temperature $T = 0.1T_c$. Shown are the normal and superconducting state curves (red and blue, respectively). ω_p is the plasma frequency. The $\alpha^2F(\omega)$ spectrum from Fig. 1 is shown shifted to the right along the frequency axis by $2\Delta_0$.

impurity scattering rate of 20 meV which is reduced by a $1 + \lambda$ factor [24] to make the half-width on the Drude conductivity to be about 7.5 meV in this case. It should be remarked that the behavior seen here due to the clean limit is quite different from what is found for conventional superconductors, such as Pb [24], which are in the dirty limit. The high energy scale of the superconducting gap contributes to sulfur hydride being in the clean limit and showing strong Holstein structure.

In summary, using three different electron-phonon spectral densities now available in the literature which are based on density functional band structure computations for H_3S under 200 GPa of pressure, we have verified that all give spectra that are near optimum for T_c. More specifically all have a characteristic phonon energy $\omega_{\ln}$ of Eliashberg theory which falls near the maximum of its own functional derivative of T_c with respect to $\alpha^2F(\omega)$. Given that the functional derivative $\delta T_c/\delta\alpha^2F(\omega)$ displays a very broad maximum, a significant distribution of phonon energies about $\omega_{\ln}$ does not deplete T_c much. For example, in the case of the $\alpha^2F(\omega)$ provided by Errea *et al.* [3] including anharmonicity, the value of T_c obtained falls only 8% below its theoretical absolute maximum for any distribution of phonon energies keeping the area under the spectral density fixed.

In Eliashberg theory, it was found that a critical parameter which measures coupling strength is the dimensionless ratio $T_c/\omega_{\ln}$. For small values of this ratio BCS theory is recovered while strong coupling corrections to the universal dimensionless ratio of BCS increase with increasing value of $T_c/\omega_{\ln}$. For H_3S, one finds a value near 0.13 which is close to that found in Pb, Nb_3Sn, and others. It corresponds to the case where $\omega_{\ln}$ is close to the maximum in the functional derivative $T_c/\omega_{\ln} \approx 7$ and hence accounts for the near optimization of the spectrum. This also implies that the thermodynamic properties of H_3S will be close to those of Pb and Nb_3Sn. This does not imply, however, that other properties of their superconducting state will be similar. As an example, optical properties in H_3S will be very different from those in other conventional superconductors which are in the dirty (impurity-dominated) limit [24]. Instead, because of the very large energy scale associated with its phonons and its superconducting gap value, H_3S is in the clean (phonon-dominated) regime. To be more precise, the absorptive part of the ac longitudinal conductivity $\mathrm{Re}\sigma_{xx}(\Omega)$ as a function of photon energy Ω will show two distinct and separate regimes. At the energy of twice the gap, the regime remains impurity dominated and there is a very sharp rise in absorption at $\Omega = 2\Delta$. but this is followed by dominant phonon-assisted absorption structures extending to many times 2Δ which is usually referred to as the clean limit regime because residual impurity scattering plays no significant role. This region provides a detailed picture of the pairing glue. Consequently, optics can be used to provide information not only on the existence of superconductivity but also of the driving mechanism.

We thank T. Timusk for discussions, and B. Pavlovic and C. Tabert for assistance with figures. This work has been supported by the Natural Sciences and Engineering Research Council (NSERC) of Canada and, in part, by the Canadian Institute for Advanced Research (CIFAR).

[1] A. P. Drozdov, M. I. Eremets, and I. A. Troyan, arXiv:1412.0460.

[2] D. Duan, Y. Liu, F. Tian, D. Li, X. Huang, Z. Zhao, H. Yu, B. Liu, W. Tian, and T. Cui, Sci. Rep. **4**, 6968 (2014).

[3] I. Errea, M. Calandra, C. J. Pickard, J. Nelson, R. J. Needs, Y. Li, H. Liu, Y. Zhang, Y. Ma, and F. Mauri, Phys. Rev. Lett. **114**, 157004 (2015).

[4] J. A. Flores-Livas, A. Sanna, and E. K. U. Gross, arXiv:1501.06336.

[5] N. Bernstein, C. S. Hellberg, M. D. Johannes, I. I. Mazin, and M. J. Mehl, Phys. Rev. B **91**, 060511 (2015).

[6] D. A. Papaconstantopoulos, B. M. Klein, M. J. Mehl, and W. E. Pickett, Phys. Rev. B **91**, 184511 (2015).

[7] J. E. Hirsch and F. Marsiglio, Physica C **511**, 45 (2015).

[8] R. Akashi, M. Kawamura, S. Tsuneyuki, Y. Nomura, and R. Arita, arXiv:1502.00936.

[9] J. P. Carbotte, Rev. Mod. Phys. **62**, 1027 (1990).

[10] See Supplemental Material at http://link.aps.org/supplemental/10.1103/PhysRevB.91.220507 for a comparison with other $\alpha^2F(\omega)$ spectra for H_3S and to see the optical conductivity curves at temperatures closer to T_c.

[11] P. B. Allen and R. C. Dynes, Phys. Rev. B **12**, 905 (1975).

[12] W. L. McMillan, Phys. Rev. **167**, 331 (1968).

[13] F. Marsiglio, T. Startseva, and J. P. Carbotte, Phys. Lett. A **245**, 172 (1998).

[14] B. Mitrovic and J. P. Carbotte, Solid State Commun. **40**, 249 (1981).

[15] J. P. Carbotte, Sci. Prog. **71**, 329 (1987).

[16] C. R. Leavens, Solid State Commun. **17**, 1499 (1975).

[17] C. R. Leavens and J. P. Carbotte, J. Low Temp. Phys. **14**, 195 (1974).

[18] B. Mitrović, H. G. Zarate, and J. P. Carbotte, Phys. Rev. B **29**, 184 (1984).

[19] B. T. Geilikman and V. Z. Kresin, Fiz. Tverd. Tela (Leningrad) **1**, 3294 (1965) [Sov. Phys. -Solid State **7**, 2659 (1966)].

[20] F. Marsiglio and J. P. Carbotte, Phys. Rev. B **33**, 6141 (1986).

[21] R. Akis, J. P. Carbotte, and T. Timusk, Phys. Rev. B **43**, 12804 (1991).

[22] J. P. Carbotte, E. Schachinger, and D. N. Basov, Nature (London) **401**, 354 (1999).

[23] J. P. Carbotte, T. Timusk, and J. Hwang, Rep. Prog. Phys. **74**, 066501 (2011).

[24] T. Mori, E. J. Nicol, S. Shiizuka, K. Kuniyasu, T. Nojima, N. Toyota, and J. P. Carbotte, Phys. Rev. B **77**, 174515 (2008).